Soil Biology and Biochemistry 156 (2021) 108211

Contents lists available at ScienceDirect

Soil Biology and Biochemistry

journal homepage: http://www.elsevier.com/locate/soilbio

The microplastisphere: Biodegradable microplastics addition alters soil microbial community structure and function

Jie Zhou [a,b,1], Heng Gui [c,d,1], Callum C. Banfield [b], Yuan Wen [a], Huadong Zang [a,*], Michaela A. Dippold [b], Adam Charlton [e], Davey L. Jones [f,g]

[a] College of Agronomy and Biotechnology, China Agricultural University, Beijing, China
[b] Biogeochemistry of Agroecosystems, Department of Crop Sciences, University of Goettingen, Goettingen, Germany
[c] CAS Key Laboratory for Plant Diversity and Biogeography of East Asia, Kunming Institute of Botany, Chinese Academy of Science, Kunming, China
[d] Centre for Mountain Futures (CMF), Kunming Institute of Botany, Chinese Academy of Science, Kunming, Yunnan, China
[e] BioComposites Centre, Bangor University, Bangor, Gwynedd, LL57 2UW, UK
[f] School of Natural Sciences, Bangor University, Bangor, Gwynedd, LL57 2UW, UK
[g] Soils West, UWA School of Agriculture and Environment, The University of Western Australia, Perth, WA 6009, Australia

ARTICLE INFO

Keywords:
Enzyme activity
Microbial growth
Microplastic pollution
Soil organic matter
C turnover
Sequencing

ABSTRACT

Plastics accumulating in the environment, especially microplastics (defined as particles <5 mm), can lead to a range of problems and potential loss of ecosystem services. Polyhydroxyalkanoates (PHAs) are biodegradable plastics used in mulch films, and in packaging material to minimize plastic waste and to reduce soil pollution. Little is known, however, about the effect of microbioplastics on soil-plant interactions, especially soil microbial community structure and functioning in agroecosystems. For the first time, we combined zymography (to localize enzyme activity hotspots) with substrate-induced growth respiration to investigate the effect of PHAs addition on soil microbial community structure, growth, and exoenzyme kinetics in the microplastisphere (i.e. interface between soil and microplastic particles) compared to the rhizosphere and bulk soil. We used a common PHAs biopolymer, poly (3-hydroxybutyrate-*co*-3-hydroxyvalerate) (PHBV) and showed that PHBV was readily used by the microbial community as a source of carbon (C) resulting in an increased specific microbial growth rate and a more active microbial biomass in the microplastisphere in comparison to the bulk soil. Higher β-glucosidase and leucine aminopeptidase activities (0.6–5.0 times higher V_{max}) and lower enzyme affinities (1.5–2.0 times higher K_m) were also detected in the microplastisphere relative to the rhizosphere. Furthermore, the PHBV addition changed the soil bacterial community at different taxonomical levels and increased the alpha diversity, as well as the relative abundance of *Acidobacteria* and *Verrucomicrobia* phyla, compared to the untreated soils. Overall, PHBV addition created soil hotspots where C and nutrient turnover is greatly enhanced, mainly driven by the accelerated microbial biomass and activity. In conclusion, microbioplastics have the potential to alter soil ecological functioning and biogeochemical cycling (e.g., SOM decomposition).

1. Introduction

Synthetic polymers are widely used in our daily lives, and more than 280 million tons of plastics are produced annually (Duis and Coors, 2016; Sintim and Flury, 2017). Despite the remarkable benefits of plastics to society, there are increasing concerns associated with the vast amount of plastic entering our environment and its resistance to degradation (Rochman, 2018). These concerns are supported by estimates that >30% of the world's plastic waste is disposed of inappropriately, with most of it ultimately ending up in soil (Jambeck et al., 2015; Weithmann et al., 2018). In soil, larger plastic debris often becomes fragmented into smaller pieces by biota and physical disturbance known as microplastics (mean diameter < 5 mm). They have received increased attention globally due to their potential to cause environmental damage (Rillig, 2012; de Souza Machado et al., 2019). A promising approach to overcome the accumulation of microplastics in soil is to replace traditional petroleum-based plastics with biodegradable bioplastics like polyhydroxyalkanoates (PHAs; Gross and Kalra,

* Corresponding author.
E-mail address: zanghuadong@cau.edu.cn (H. Zang).
[1] These authors contributed equally to this study.

https://doi.org/10.1016/j.soilbio.2021.108211
Received 27 October 2020; Received in revised form 27 February 2021; Accepted 6 March 2021
Available online 11 March 2021

2002; Volova et al., 2017). PHAs account for 5.6% of the global production capacity for biodegradable polymers, and represent the second fastest growing group in the market sector since 2014 (Haider et al., 2019). Even though PHAs are used in an attempt to decrease microplastic residues in terrestrial ecosystems, and praised as promising alternatives for a diverse range of applications (e.g., mulch films for agriculture), the potential environmental consequences of PHAs have not yet been thoroughly studied.

Unlike petroleum-based microplastics, which biodegrade extremely slowly, PHAs can be broken down by a range of organisms and are not thought to produce any harmful by-products (Volova et al., 2017; Haider et al., 2019; Sander et al., 2019). Given their biological origin, they are considered C neutral (Garrison et al., 2016), although this assumes that they do not induce positive priming of soil organic matter (SOM). Furthermore, they are thought to not enhance N_2O and CH_4 emissions which might offset these benefits. Given that PHAs are C-rich but nutrient-poor (i.e. no N and P; Gross and Kalra, 2002; Volova et al., 2017), they may alter microbial community composition and functioning during degradation. Since the decomposition of C-rich residues is associated with N and P immobilization, subsequent plant growth may also be affected due to the increased competition between plants and soil microorganisms for nutrients (Qi et al., 2018, 2020b; Song et al., 2020; Zang et al., 2020). In response to the additional C supplied from PHAs breakdown, the turnover of native SOM may be stimulated due to the altered metabolic status of the microbial community (Kuzyakov, 2010; Zang et al., 2017), and thus influence soil C and nutrient cycling. PHAs are also naturally present in soil being produced as storage compounds by the bacterial community (Mason-Jones et al., 2019). Given that bacteria are more sensitive to environmental changes (e.g. increased labile C) compared to fungi (Barnard et al., 2012), soil bacteria may have a stronger response due to the increased C availability through PHAs breakdown. This will lead to significant long-term impacts on a range of soil ecosystem services (e.g., C storage, nutrient cycling, and pollutant attenuation; Zang et al., 2018). Although recent studies revealed that microplastics may have divergent influences on soil microbial communities and enzyme activities, e.g., activation (Liu et al., 2017; de Souza Machado et al., 2019), suppression (Fei et al., 2020), or remaining unchanged (Zang et al., 2020), the effect of microbioplastics on soil microorganisms remains poorly understood. Therefore, it is vital to investigate how biodegradable microplastics affect microbial functions and below-ground C processes (Zang et al., 2019, 2020; Qi et al., 2020a).

Similar to plant-soil interactions in the rhizosphere, the main processes affected by microplastic input may occur at the soil-plastic interface (here defined as the microplastisphere). We hypothesize that these interactions are stimulated by the input of bioavailable C present in microbioplastics (i.e. increased microbial activity, attract or favor specific bacterial taxa, and interfere with belowground plant-microorganisms interactions) leading to the formation of microbial hotspots in soil, similar to those seen in the rhizosphere (Kuzyakov and Blagodatskaya, 2015; Zang et al., 2016; Zhou et al., 2020b). Following PHAs addition, we predict that changes in the soil physico-chemical properties will only occur close to the microplastic particles, with changes in the (non-hotspot) bulk soil likely to be minor (Zettler et al., 2013; Huang et al., 2019). The specific niches of the microorganisms in the microplastisphere are of ecological relevance, given that most agricultural soils are contaminated by microplastics (Steinmetz et al., 2016; Qi et al., 2020a). However, it still remains unclear how PHAs affect soil microbial communities in hotspots and, thus, alters soil C and nutrient cycling.

Here, for the first time, we coupled zymography, a method to accurately locate microbial hotspots (Hoang et al., 2020; Zhang et al., 2020), the kinetics of exoenzyme activities involved in C, N, and P cycling, microbial growth, and bacterial community structure to evaluate microbial functions, as well as soil process in hotspots (rhizosphere and microplastisphere) and bulk soil. Poly (3-hydroxybutyrate-*co*-3-hydroxyvalerate) (PHBV) represents a commercially available copolymer used for mulch film production. Compared to PHB, it has higher flexibility, thermal stability, and processibility due to the monomeric composition, which makes it a promising example of PHAs (Table S1; Jiang et al., 2009; Bugnicourt et al., 2014). Therefore, we aimed to 1) identify microbial hotspots *in situ* in soil treated with PHBV; 2) investigate the effect of biodegradable microplastics on microbial growth and enzyme kinetics; 3) evaluate changes in the bacterial community structure and function in the microplastisphere and rhizosphere. We hypothesized that: 1) the labile C in PHBV will greatly alter soil bacterial community structure and functioning compared to the rhizosphere and bulk soil, and 2) the microplastisphere contains microorganisms with a high growth rate and enzyme activity in comparison to rhizosphere and bulk soil.

2. Materials and methods

2.1. Site description and sampling

Soil samples were taken from the Ap horizon (0–20 cm) of an experimental field at the Reinshof Research Station of the Georg-August University of Göttingen, Germany (28°33′26″N, 113°20′8″E). This experimental site was established more than 40 years ago and the farming history is well documented. No plastic mulch has ever been applied, and no plastic pollution has been recorded for the site. The soil was air-dried, sieved (<2 mm), and mixed to achieve a high degree of homogeneity and to reduce the variability among replicates. Fine roots and visible plant residues were carefully removed prior to use. The soil contained 1.3% total C, 0.14% total N, and had a pH of 6.8 (Zhou et al., 2020b). Ten percent (w/w) of the soil dry weight was added as poly (3-hydroxybutyrate-*co*-3-hydroxyvalerate) ($[COCH_2CH(CH_3)O]m[COCH_2CH(C_2H_5)O]_n$) (PHBV). PHBV was obtained in a pelletized form from the Tianan Biologic Materials Company Ltd., Beilun, Ningbo, China. PHBV represents one of the most widespread and best characterized members of the PHA family (Bugnicourt et al., 2014). It is a 100% biobased thermoplastic linear aliphatic (co-)polyester obtained from the copolymerization of 3-hydroxybutanoic acid and 3-hydroxypentanoic acid which are produced through the bacterial fermentation of sugars and lipids (Zinn et al., 2001). Most of the PHBV is composed of hydroxybutyrate, however, a small fraction of hydroxyvalerate is present in its polymeric backbone (Rivera-Briso and Serrano-Aroca, 2018). This type and amount of highly crystalline plastic were chosen to simulate the localized disposal of bioplastics in agricultural soils (e.g., ploughing in of mulch film residues at the end of the field season) and was based on field investigations and a review of the literature (Fuller and Gautam, 2016; Qi et al., 2020a). We added very high amounts of microplastic to reflect soil hotspots with higher contamination levels (1–20%).

2.2. Experimental design

A mesocosm experiment with a completely randomized design and four replicates was set up in a climate-controlled room. For the PHBV addition treatment, 400 g soil and PHBV were mixed homogeneously and then put in a rhizobox (10 × 10 × 4 cm; Qiangsheng Co., Ltd. Heibei, China). The control treatment contained soil (400 g) without PHBV, but with a comparable soil disturbance. The soil bulk density was maintained at 1.2 g cm^{-3} for all rhizoboxes. Prior to use, the soil was pre-incubated under field-moist (25% v/v) conditions in a greenhouse for one week to allow the soil to equilibrate. Before planting, wheat (*Triticum aestivum* L.) seeds were sterilized in 10% H_2O_2 for 10 min, then rinsed with deionized water and germinated on wet filter paper. Five days after germination, seedlings were transplanted in all rhizoboxes (one seedling per rhizobox), and then moved to the climate-controlled chamber (day/night regime of 14 h/24 °C and 10 h/14 °C, respectively). The relative humidity in the chamber was kept at 40% and the

plants received 800 μmol m^{-2} s^{-1} photosynthetic active radiation (PAR) at canopy height (Zhou et al., 2020b). Plants were watered every three days and the soil moisture was maintained at a gravimetric water content of 25% throughout the experiment by weighing the rhizoboxes.

2.3. Hotspot identification

At 24 days after transplanting, zymography was used to visualize the spatial distribution of three hydrolytic enzymes (Razavi et al., 2016). B-glucosidase, acid phosphatase, and leucine-aminopeptidase play major roles in cellulose, organic phosphate, and protein degradation (Lopez-Hernandez et al., 1993; Lammirato et al., 2010). They reflect key enzymes related to soil C, P and N cycle, respectively (German et al., 2011). Polyamide membrane (0.45 μm mesh size, Tao yuan, China) were saturated with 4-methylumbelliferyl (MUF) or 7-amido-4-methylcoumarin (AMC) based substrate to visualize the specific enzymes. Each substrate was separately dissolved in 10 mM MES and TRIZMA buffer for MUF and AMC, respectively. The saturated membranes were placed on soil surfaces and covered with aluminum foil to avoid evaporation and moisture changes during the incubation period (Hoang et al., 2020). After incubation for 1 h, the membranes were carefully peeled off the soil surface and any attached soil particles were gently removed with tweezers and a soft brush (Razavi et al., 2016). Enzyme detection sequences followed as: β-glucosidase, acid phosphatase, leucine-aminopeptidase activity, with 1 h interval after each zymography. The gray scale values transferred to the enzyme activities was calibrated using membranes (2 × 2 cm) saturated with a range of concentrations of corresponding products, i.e. MUF and AMC (0, 0.01, 0.2, 0.5, 1, 2, 5 mM).

The zymograms were transferred into a 16-bit gray scale by ImageJ with a correction for environmental variations and camera noise (Razavi et al., 2016). The calibration equation obtained for each enzyme was used to convert gray values of each zymography pixel into enzyme activities (Hoang et al., 2020). Enzyme activities exceeding 25% of mean corresponding activity of the whole soil were defined as hotspots (Zhang et al., 2020). Specifically, soil with a high color intensities (shown here in dark red) represent microbial hotspots, while low intensities (shown here in dark blue) indicate (non-hotspot) bulk soil on the zymograms (Fig. 1; Hoang et al., 2020). Given the hotspots in the control and PHBV-treated soil were detected at a distance of 1.5–2 mm from the roots and microplastics, the hotspots in the control and PHBV-treated soil were identical to the rhizosphere and microplastisphere zones, respectively (Fig. 1). After collecting soil from hotspots and bulk soil, a total of 16 samples [2 treatments (without and with PHBV) × 2 microsites from each treatment (hotspots and bulk soil) × 4 replicates] were obtained.

2.4. Plant and soil sampling

At 25 days after transplanting, the shoots were cut off at the base of the stem and the roots were collected separately. For precise localized sampling, soil particles were carefully collected using needles (tip 1.5 mm) directly from the hotspots (rhizosphere and microplastisphere) identified by zymography (Fig. 1). Bulk soil was collected in a similar way. Once collected, soil samples (hotspots and bulk soil) were separated into two sub-samples. One sub-sample was stored at −80 °C to

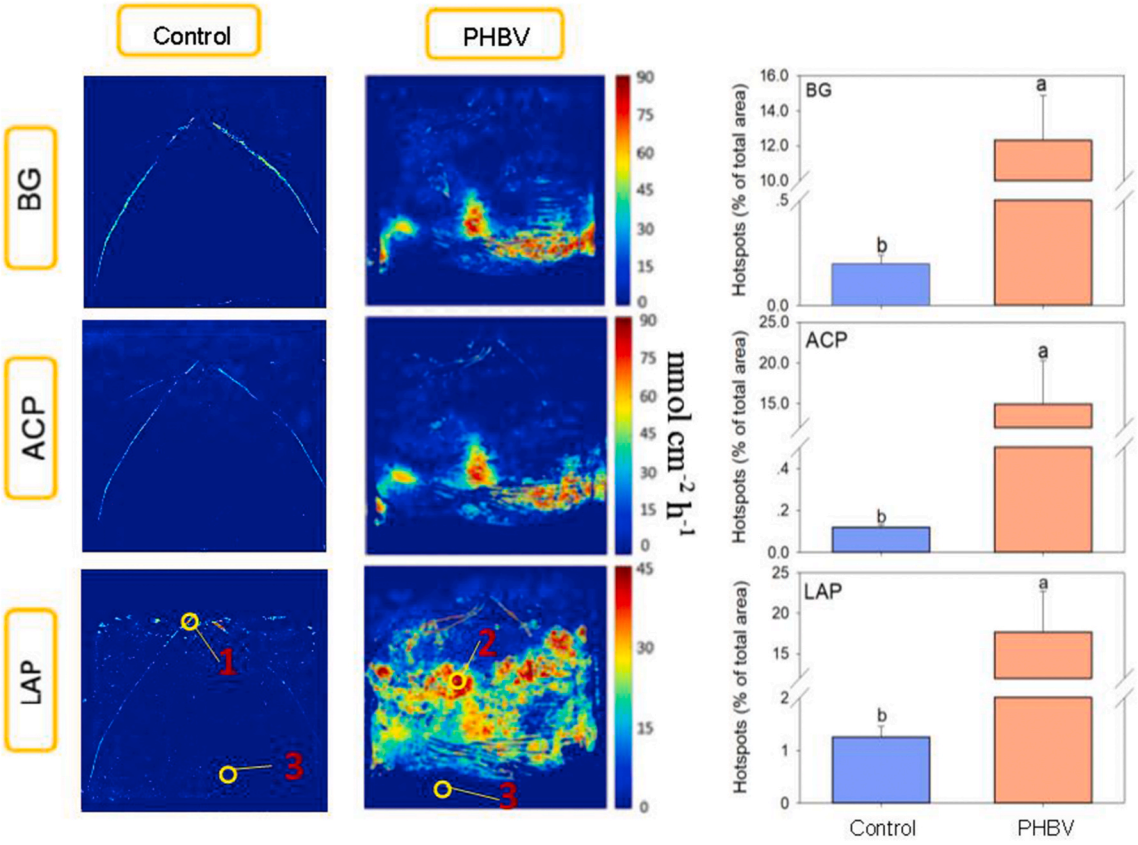

Fig. 1. Zymograms and hotspots of β-glucosidase (BG), acid phosphatase (ACP) and leucine aminopeptidase (LAP) in untreated soil (Control) and soil to which the bioplastic poly(3-hydroxybutyrate-*co*-3-hydroxyvalerate) (PHBV) was added. The color intensity is proportional to the respective enzyme activity (nmol cm^{-2} h^{-1}). The zymograms are representative of 4 independent replicates. The corresponding area of hotspots relative to the total area of the rhizobox for each enzyme is shown in the right-hand panel. Values are means (±SE) of four replicates. Different letters show significant differences between treatments ($p < 0.05$). Here, 1, 2, 3 indicate rhizosphere, microplastisphere, and bulk soil. (For interpretation of the references to color in this figure legend, the reader is referred to the Web version of this article.)

analyze the bacterial community structure, while the other sub-sample was used to measure enzyme kinetics and the kinetics of substrate-induced growth respiration directly. After removal of the hotspot samples and bulk soil, the remaining soil in the rhizobox was mixed and then stored at 4 °C to measure microbial biomass N, dissolved organic C and N. Shoots and roots were oven-dried (60 °C, 5 days) and then weighed.

Soil microbial biomass N (MBN) was extracted with K_2SO_4 (32 mL, 0.05 M), and calculated with a corresponding K_{EN} factor of 0.45 according to Wen et al. (2020). Briefly, the fresh soil was homogenized and 8 g sub-sample of the soil were extracted with 32 mL 0.05 M K_2SO_4. Another 8 g sub-sample of the soil was fumigated with chloroform for 24 h and then extracted in the same way. Total C and N in extracts were measured on a 2100 N/C analyzer (Analytik Jena GmbH, Jena, Germany). The non-fumigated extractions were used as a measure for dissolved organic C (DOC) and N (DON).

2.5. Enzyme kinetics

The activity of the exoenzymes β-1,4-glucosidase (BG) (EC 2.2.1.21), leucine aminopeptidase (LAP) (EC 3.4.11.1), and acid phosphatase (ACP) (EC 3.1.3.2) were determined by the 4-methylumbelliferyl (MUF)-based and 7-amido-4-methylcoumarin (AMC)-based artificial substrates (Marx et al., 2001; Wen et al., 2019). Briefly, 0.5 g soil was mixed with 50 mL sterile water and then shaking for 30 min. After 2 min low-energy sonication (40 J s^{-1}) by ultrasonic disaggregation, 50 μl of the soil suspension, 50 μl of corresponding buffer (MES or TRIZMA) and 100 μl of the corresponding substrates at concentrations of 2, 5, 10, 20, 50, 100 and 200 μmol l^{-1} were pipetted into 96-well black microplates (Brand® plates pureGrade, Sigma-Aldrich, Germany). The Victor 1420-050 Multi label Counter (PerkinElmer, USA) was used to measure the fluorescence at an excitation wavelength of 355 nm and an emission wavelength of 460 nm. Enzyme activities were taken at four times (0, 30 min, 1 h and 2 h), and was expressed as nmol g^{-1} soil h^{-1}.

To calculate key parameters describing the enzyme kinetics, we fitted a Michaelis-Menten equation to the experimental data (Marx et al., 2001):

$$V = \frac{V_{max} \times [S]}{K_m + [S]} \quad (1)$$

where V is the enzymatically mediated rate of reaction, V_{max} is the maximal rate of reaction, K_m (Michaelis constant) is the substrate concentration at ½V_{max} and S is substrate concentration. The substrate turnover time (T_t) was calculated according to the following equation: T_t (hours) = (K_m + S)/V_{max}, where S is the substrate concentration (200 μmol l^{-1}). The catalytic efficiency of enzymes (K_a) was calculated by the ratio of V_{max} and K_m (Hoang et al., 2020). The microbial metabolic limitation was quantified by calculating the vector lengths and angles of enzymatic activity for all data based on untransformed proportional activities (e.g. (BG):(BG + LAP), (BG):(BG + ACP)) (Moorhead et al., 2016).

2.6. Kinetics of substrate-induced growth respiration

The substrate-induced growth respiration (SIGR) approach was used to distinguish total and active biomass fractions, as well as microbial specific growth rate and lag-time before growth (Zhang et al., 2020; Zhou et al., 2020a). It should be noted that although C substrate addition is required for the SIGR approach, all kinetic parameters analyzed by SIGR represent the intrinsic features of dominating microbial populations before substrate addition (Blagodatskaya et al., 2010).

One gram of fresh soil was amended with a mixture containing 10 mg g^{-1} glucose, 1.9 mg g^{-1} $(NH_4)_2SO_4$, 2.25 mg g^{-1} K_2HPO_4, and 3.8 mg g^{-1} $MgSO_47H_2O$, and placed in a Rapid Automated Bacterial Impedance Technique bioanalyzer (RABIT; Microbiology International Ltd, Frederick, MD, USA), for measuring CO_2 production at room temperature (22 °C). Firstly, we pre-incubated 16 samples from hotspots and bulk soil with and without PHBV amendment for 2 days at 45% water holding capacity (WHC) to minimize the effect of sampling disturbance. To measure substrate-induced respiration, a mixture of glucose and nutrients was added and the samples were further incubated for 5 day at 75% WHC (Blagodatskaya et al., 2010; Zhou et al., 2020a). The evolving CO_2 was trapped in a KOH solution where the impedance of the solution was continuously measured. The average value of CO_2 emission during the 3 h before and after adding substrates were taken as basal respiration (BR), and substrate-induced growth respiration (SIGR).

Microbial respiration in glucose amended soil was used to calculate the following kinetic parameters: the microbial maximal specific growth rate (μ), the growing microbial biomass (GMB) that capable for immediate growth on glucose, the total microbial biomass (TMB) responding by respiration to glucose addition, and the lag period (T_{lag}).

Microbial maximal specific growth rate μ was used as an intrinsic property of the microbial population to estimate the prevailing growth strategy of the microbial community. According to Blagodatskaya et al. (2010), higher μ reflects relative domination or shift towards fast-growing *r*-strategists, while lower μ values show relative domination or shift towards slow-growing *K*-strategists.

Considering that PHBV is partially soluble in chloroform at 30 °C (Jacquel et al., 2007), the microbial biomass we measured by chloroform-fumigation extraction might contain a minor contribution from PHBV degradation during fumigation. Therefore, microbial biomass C (MBC) was determined using the initial rate of substrate-induced respiration after substrate addition according to the equation of Blagodatskaya et al. (2010):

$$\text{MBC (μg } g^{-1} \text{ soil)} = (\text{μl } CO_2\ g^{-1} \text{ soil } h^{-1}) \times 40.04 \quad (2)$$

2.7. Soil bacterial community structure

2.7.1. Soil genomic DNA extraction, PCR amplification and illumina sequencing

Total DNA was extracted from 0.5 g soil for each treatment using the Mo Bio PowerSoil DNA isolation kit (Qiagen Inc., Carlsbad, CA, USA) according to the manufacturer's instructions. After extraction, the quality and concentration of DNA were tested using a NanoDrop ND 200 spectrophotometer (Thermo Scientific, USA). According to the concentration, all DNA samples were diluted to 1 ng μl^{-1} before PCR amplification. We note that the DNA extracted from control hotspots leaked out during shipping for sequencing analysis, causing the DNA concentration to drop under the detection threshold. Therefore, the samples from this treatment could not be determined.

The V4 and V5 variable region of the bacterial 16S rRNA gene were amplified using the primers 515F (5′-CCATCTCATCCCTGCGTGTCTCCGAC-3′) and 907R (5′-CCTATCCCCTGTGTGCCTTGGCAGTC-3′). The polymerase chain reaction (PCR) amplification mixture was prepared with 1 μl purified DNA template (10 ng), 5 μl 10 × PCR buffer, 2.25 mmol l^{-1} $MgCl_2$, 0.8 mmol l^{-1} deoxyribonucleotide triphosphate (dNTP), 0.5 μmol l^{-1} of each primer, 2.5 U Taq DNA polymerase, and sterile filtered ultraclean water to a final volume of 50 μl. All the reactions were carried out in a PTC-200 thermal cycler (MJ Research Co., NY, USA). The PCR cycles included a 4 min initial denaturation at 94 °C, followed by 30 cycles of denaturation at 94 °C for 1 min, annealing at 53 °C for 30 s, extension at 72 °C for 1 min, and a 5-min final elongation step at 72 °C. The PCR products were quality-screened and purified by Qiagen Gel Extraction kit (Qiagen, Hilden, Germany). Next, all the amplicons were sequenced on the Illumina Miseq PE250 platform at Novogene Biotech Co., Ltd., Beijing, China. All the sequences have been submitted to NCBI SRA data repository under the Accession No. PRJNA648785.

2.7.2. 16S gene sequences processing

Briefly, de-noising and chimera analysis conducted with the AmpliconNoise and UCHIME algorithms were used to reduce sequence errors (Vargas-Gastelum et al., 2015). Furthermore, quality trimming was conducted to remove unwanted sequences shorter than 200 bp and reads containing ambiguous bases and with homopolymers longer than eight bases. The remaining sequences were used to identify the unique sequences by aligning with the SILVA reference database (v.128) (Quast et al., 2013). Within unique sequences, the UCHIME tool was applied to remove chimeras. Then, "Chloroplast", "Mitochondria", or "unknown" were identified and removed from the dataset. Subsequently, after calculating the pairwise distance and generating the distance matrix, a 97% identity threshold was used to cluster sequences into Operational Taxonomic Units (OTUs) according to the UCLUST algorithm (Edgar et al., 2011). The most abundant sequence in each OTU was picked as the representative sequence. For each representative sequence, the SILVA reference database (v.128) was applied to annotate the taxonomic information using RDP classifier algorithm (Wang et al., 2007).

2.8. Statistical analysis

The experiment was carried out with four replicates for each parameter. All values presented in the figures are means ± standard errors of the means (mean ± SE). The enzyme kinetic parameters (V_{max} and K_m) were fitted via the non-linear regression routine of SigmaPlot (version 12.5; Systat Software, Inc., San Jose, CA, USA). The DNA data were rarefied to an equal depth within the minimum observed sample size across all the samples. The following six parameters, namely Richness, Pielou, Chao1, Shannon, Simpson, and abundance-based coverage (ACE), were calculated to describe the alpha diversity of the soil bacterial community based on OTU abundance. The calculation was conducted in QIIME 2 and the illustration was performed by R software (Ver. 3.2) using the packages "ggplot2" and "metacoder".

Prior to the analysis of variance (ANOVA), the data were tested for normality (Shapiro-Wilk, $p > 0.05$) and homogeneity of variance (Levene-test, $p > 0.05$). Any dataset that was not normally distributed was root square or $\log_{10}$-transformed to conform with the assumption of normality before further statistical analysis. For alpha diversity indices that did not conform to the assumption of normality, the nonparametric Kruskal-Wallis H-Test was applied to determine whether there were significant differences in alpha diversity among different treatments.

3. Results

3.1. Effect of PHBV on plant and soil properties

The mean plant biomass was 0.24 g pot^{-1} without microplastics addition (Table 1). However, PHBV addition ultimately resulted in plant death after 25 days. PHBV addition greatly increased the soil microbial biomass and dissolved organic C content ($p < 0.05$, Table 1). MBC and DOC were 12 and 54 times higher in the PHBV-treated than in the control soil, respectively. Additionally, MBN was 45% higher in the PHBV-treatment in comparison to the control, whereas DON decreased by 66% compared to the control soil.

Table 1
Plant biomass, microbial biomass carbon (MBC) and nitrogen (MBN), and dissolved organic carbon (DOC) and nitrogen (DON) in untreated soil (Control) and soil to which the bioplastic poly(3-hydroxybutyrate-*co*-3-hydroxyvalerate) (PHBV) was added. Values are means (±SE) of four replicates. Letters show significant differences between treatments ($p < 0.05$). MBC was calculated by substrate-induced growth respiration (according to Eq. (2)), MBN was measured by chloroform-fumigation extraction, DOC and DON were determined by non-fumigated extractions.

Treatment	Plant biomass (g DM pot^{-1})	MBC (mg kg^{-1})	MBN (mg kg^{-1})	DOC (mg kg^{-1})	DON (mg kg^{-1})
Control	0.24 ± 0.02	131 ± 23b	20.6 ± 3.4b	163 ± 20b	93.9 ± 5.5a
PHBV	n.d.	1723 ± 625a	30.4 ± 5.6a	9049 ± 889a	32.3 ± 5.2b

n.d.: no data due to plant death.

3.2. Effect of PHBV on soil enzyme activities

The maximum potential enzyme activities (V_{max}) were 60% and 5-folds higher for β-glucosidase and leucine aminopeptidase in the microplastisphere than in the rhizosphere, respectively ($p < 0.05$, Fig. 2a and b). Similarly, the substrate affinities (K_m) of β-glucosidase and leucine aminopeptidase in the microplastisphere were 1.5–2 times higher in the rhizosphere, respectively ($p < 0.05$, Fig. 2b, d). The V_{max} and K_m of β-glucosidase and leucine aminopeptidase in microplastisphere were significantly higher compared to those in the PHBV-treated bulk soil ($p < 0.05$, Fig. 2). In the bulk soil, however, none of the tested enzymes were affected by PHBV addition ($p > 0.05$, Fig. 2). Furthermore, the V_{max} of β-glucosidase was positively correlated with active microbial biomass ($R^2 = 0.7$, $p < 0.05$, Fig. S4). The catalytic efficiency (V_{max}/K_m) of leucine aminopeptidase was higher in the microplastisphere than in the rhizosphere ($p < 0.05$, Fig. S2c), and the turnover time was approximately 5 times shorter in the microplastisphere than in the rhizosphere soil (Fig. S2d). However, no changes in the catalytic efficiency and turnover time for all the enzymes were found in the bulk soil between the PHBV-treated and control soil ($p > 0.05$, Fig. S2). Further, the vector angle was lowest in the microplastisphere compared to other soil samples ($p < 0.05$, Fig. S7d), indicating that microbial metabolisms may be N limited.

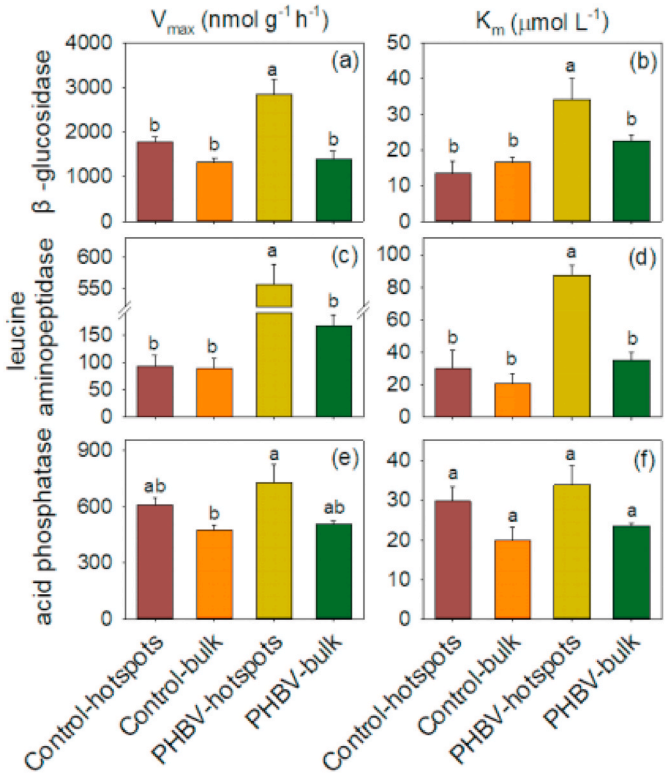

Fig. 2. Potential enzyme activities (V_{max}) and substrate affinities (K_m) of β-glucosidase (BG), leucine aminopeptidase (LAP), and acid phosphatase (ACP) in bulk and hotspots in untreated soil (Control) and soil to which the bioplastic poly(3-hydroxybutyrate-*co*-3-hydroxyvalerate) (PHBV) was added. Values are means (±SE) of four replicates. Different letters show significant differences between treatments ($p < 0.05$).

3.3. Effect of PHBV on soil microbial growth rate

Different microbial growth patterns in response to substrate addition were observed among hotspots (microplastisphere and rhizosphere) and the bulk soil with and without PHBV addition (Fig. S3). The basal respiration (BR, 45 μg C g^{-1} h^{-1}) and substrate-induced growth respiration (SIGR, 58 μg C g^{-1} h^{-1}) in the microplastisphere were 10 times and 12 times higher relative to the rhizosphere soil, respectively (Fig. 3a and b). However, the BR and SIGR in the bulk soil were not affected by PHBV addition compared to the control.

Soil respiration showed a clear response to PHBV addition both in the hotspots and in bulk soil (Fig. S3). PHBV addition decreased the maximum specific growth rate (μ) by 22% in the microplastisphere compared to the bulk soil ($p < 0.05$; Fig. 3c), whereas there was no difference in μ between the microplastisphere and the PHBV-treated bulk soil ($p > 0.05$). Despite a slower specific growth rate, a 6-fold increase in the fraction of active microbial biomass, and a four times shorter lag period was observed in the microplastisphere vs. rhizosphere soil (Fig. 3d,e,f).

3.4. Effect of PHBV on soil bacterial community composition and diversity

The dominant bacteria phyla were *Actinobacteria, Proteobacteria, Acidobacteria, Firmicutes, Bacteroidetes, Chloroflexi, Thaumarchaeota*, and *Gemmatimonadetes* in all treatment soils (Fig. 4A), which together encompassed ca. 96–98% of the bacterial reads. Although the dominant phyla in all soils were consistent, changes in the relative abundances of the dominant taxa were observed across the treatments. There was a higher abundance of *Proteobacteria* and *Acidobacteria* and a lower abundance of *Firmicutes* in soils with PHBV addition comparing with control treatment ($p < 0.05$, Fig. 4A). In the family level, the fraction of these 20 dominant families with highest relative abundance decreased after PHBV addition (Fig. 4B). Specifically, the addition of PHBV induced the decrease of *Planococcaceae, Xanthomonadaceae*, *Bacillaceae* and the increase of *Chitinophagaceae*, *Comamonadaceae* and *Oxalobacteraceae* (Fig. 4B). The detailed family level changes of bulk and hotspot soil bacterial community induced by PHBV addition were also given in Fig. 5C. Of the 3800 OTUs detected across all samples, the major numbers of OTUs ($n = 3622$) were shared by control-bulk, PHBV-bulk, and PHBV-hotspots soils, while 54 OTUs were unique to PHBV-hotspots soil and 16 OTUs were unique to the PHBV-bulk soil (Fig. 5A).

The mean values for ACE, Chao1, Richness, and Shannon indices in the PHBV-treated bulk soil increased by 10%, 11%, 16%, and 18% relative to the control soil, respectively (Fig. S5), while there were no differences between the microplastisphere and bulk soil after PHBV addition ($p > 0.05$).

4. Discussion

4.1. Effect of PHBV on plant growth

Intact PHBV and its decomposition products are thought to be of very low cytotoxicity (Napathorn, 2014). In all the rhizoboxes amended with PHBV, however, all the plants eventually died during the 4-week experiment. This is consistent with previous reports showing that degradation of conventional and bio-based microplastics might negatively affect plant growth when present in high quantities (Qi et al., 2018, 2020b; Zang et al., 2020). Given that bioplastic polymers are solely composed of C, O and H, it is likely that PHBV addition to soil induced microbial immobilization of essential nutrients (e.g., N, P) leading to increased plant stress (Volova et al., 2017; Boots et al., 2019). Such an N immobilization was further confirmed by the decreased DON but increased MBN in PHBV-added soil compared to the unamended control treatment (Table 1). This is consistent with Sander (2019) who found that microorganisms on the surface of microplastics need to acquire N from the surrounding soil to fuel growth. It also suggests that PHBV may have stimulated opportunistic plant pathogens (Matavulj et al., 1992), however, more work is required to confirm this. An alternative explanation might be that PHBV induced phytotoxicity due to acidification of the soil because of the release of high quantities of 3-hydroxybutyric acid during PHBV degradation. However, this would normally affect root growth rather than shoot growth (Lucas et al., 2008). Further, based on the degradation of other biopolymers (e.g. cellulose, proteins), it is unlikely that an accumulation of the monomer will occur due to rapid microbial consumption (Jan et al., 2009). This is

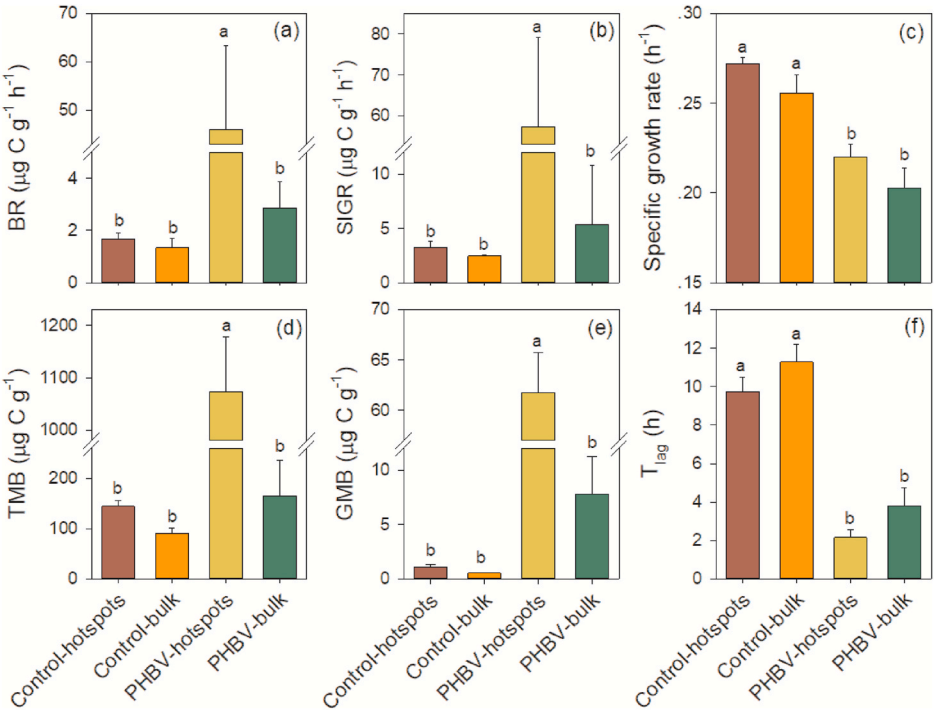

Fig. 3. Basal respiration (BR), substrate-induced growth respiration (SIGR), specific growth rate (μ), total microbial biomass (TMB), the fraction of growing microbial biomass to total microbial biomass (GMB/TMB), and their lag time in bulk and hotspots in untreated soil (Control) and soil to which the bioplastic poly(3-hydroxybutyrate-*co*-3-hydroxyvalerate) (PHBV) was added. Values are means (±SE) of four replicates. Letters show significant differences between treatments ($p < 0.05$).

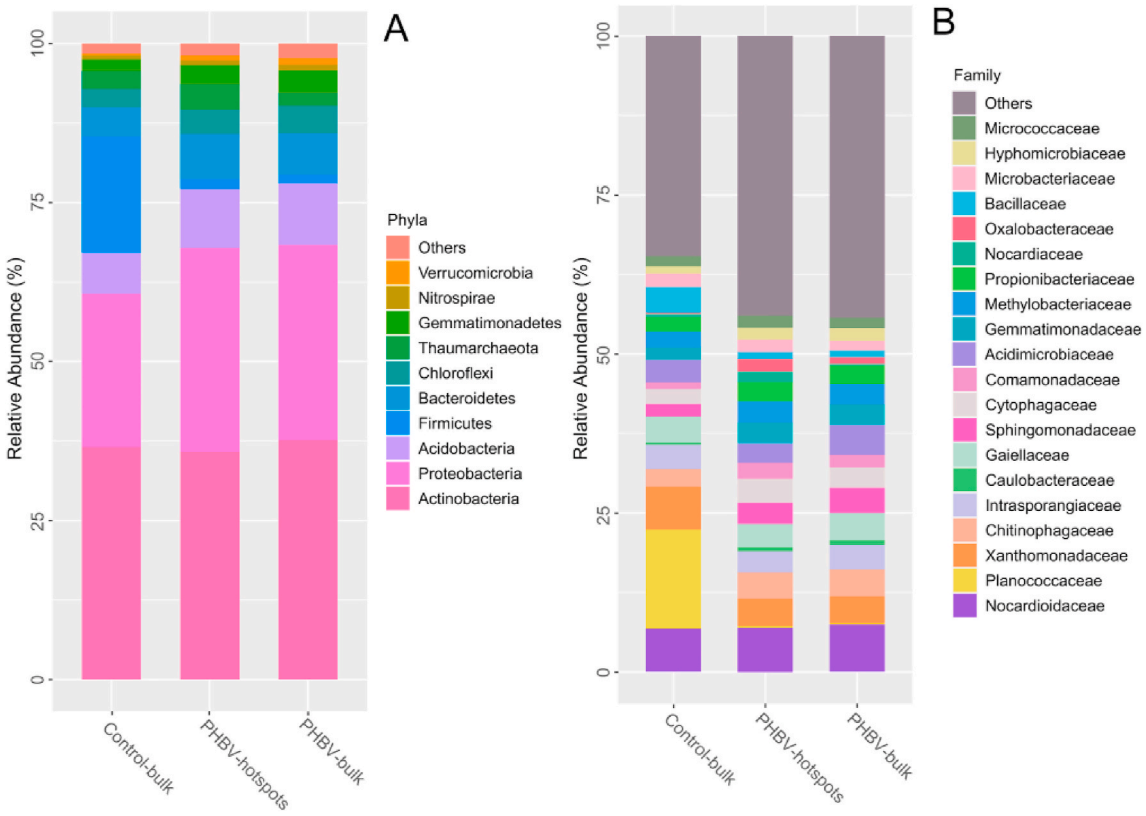

Fig. 4. Stacked bar chart of the top 10 bacterial phyla with the largest mean relative abundance in untreated soil (Control-bulk), and bulk (PHBV-bulk) and hotspots (PHBV-hotspots) soils with the bioplastic poly (3-hydroxybutyrate-*co*-3-hydroxyvalerate) (PHBV) addition (A). Stacked bar plot of the 20 families with largest mean relative abundance in all soil samples (B).

quite likely as it is a monomer which is naturally present as a microbial storage compound (Mason-Jones et al., 2019). However, it is possible that undisclosed additives or contaminants in the polymer might also have induced phytotoxicity (Zimmermann et al., 2019). Lastly, we cannot disregard other general changes in soil properties and microbial communities following PHBV addition which may also have inhibited plant growth, contributing to plant death (Saarma et al., 2003; Wen et al., 2020). We conclude, that contrary to expectation, commercially sourced PHBV was deleterious to plant growth, at least under higher contents of PHBV in the short term, as indicated by the lower seed germination over 7-days germination (Fig. S6). Further experiments are therefore needed to determine the mechanistic basis of this response.

4.2. *Effect of PHBV on soil microbial and enzymatic functional traits*

Soil enzyme production is sensitive to both energy and nutrient availability (Allison et al., 2011). This notion was supported in our study where the input of bioavailable C (i.e. degradation products of PHBV) increased enzyme activities in hotspots by up to 2 times compared to the bulk soil. This increase in microbial activity is unsurprising given that poly-3-hydroxybutyrate is a common storage compound produced by a wide range of taxonomically different groups of microorganisms, particularly in response to N deficiency and cold stress (Obruca et al., 2016). Consequently, the ability to use PHBV-C is expected to be a widespread trait within the microbial community. For C- and N-degrading enzymes, the activity difference between hotspots and the bulk soil was 2–10 times larger when PHBV was added (Fig. 2a, c), demonstrating that bioplastic incorporation into the soil directly influences C and N cycling. The higher V_{max} of β-glucosidase in the microplastisphere versus rhizosphere soil can be attributed to the faster growing biomass after PHBV addition (Fig. 3e). This is supported by the positive correlation between our measurement of the active microbial biomass and the V_{max} of β-glucosidase ($R^2 = 0.7$, Fig. S4). The increase in β-glucosidase also suggests that PHBV is stimulating the breakdown of other common soil polymers (i.e. cellulose). Further, PHBV could be broken down by depolymerases releasing hydroxybutyric acid monomers which fuel the production of energetically expensive exoenzymes (i.e. leucine aminopeptidase; Fig. 2c) capable of degrading SOM to acquire N for growth (i.e. positive priming; Zang et al., 2016; Zhou et al., 2020a, b). This was supported by a higher BR and SIGR in the microplastisphere relative to the bulk soil (Fig. 3a and b), as well as the wider ratio of DOC and DON in the PHBV-treated soil (294) than in the control soil (1.77) (Table 1). In accordance with previous studies, N limitation also induced an increase in the catalytic properties (K_a) of leucine aminopeptidase (Song et al., 2020). In line with this, the much shorter turnover time of substrates and higher K_a of leucine aminopeptidase in the microplastisphere was observed compared to the rhizosphere (Figs. S2c and d), which suggests that the community was more limited by N than P in the microplastisphere. This could be supported by lower proportional activity of C- to N-cycling enzymes but higher proportional activity of C- to P-cycling enzymes in the microplastisphere versus the rhizosphere (Fig. S7). The lower vector angle in the microplastisphere further confirmed the microbial metabolisms were likely limited by soil N. We therefore hypothesize that due to N limitation the microbial community either (i) changed the intrinsic properties of their hydrolytic enzymes to adapt to the presence of the C-rich bioplastic, and/or (ii) that PHBV induced a shift in the soil microbial community and thus the types of enzymes being produced (Kujur and Patel, 2013). Overall, we conclude that N limitation is connected to microbial N immobilization due to stimulated microbial growth after C supply from PHBV. The C input stemming from the catabolism of PHBV will increase microbial biomass and intensify the N limitation. This was supported by the increased MBC and enzyme activities (especially N related), as well as the shift in enzymatic stoichiometric ratio and bacterial community.

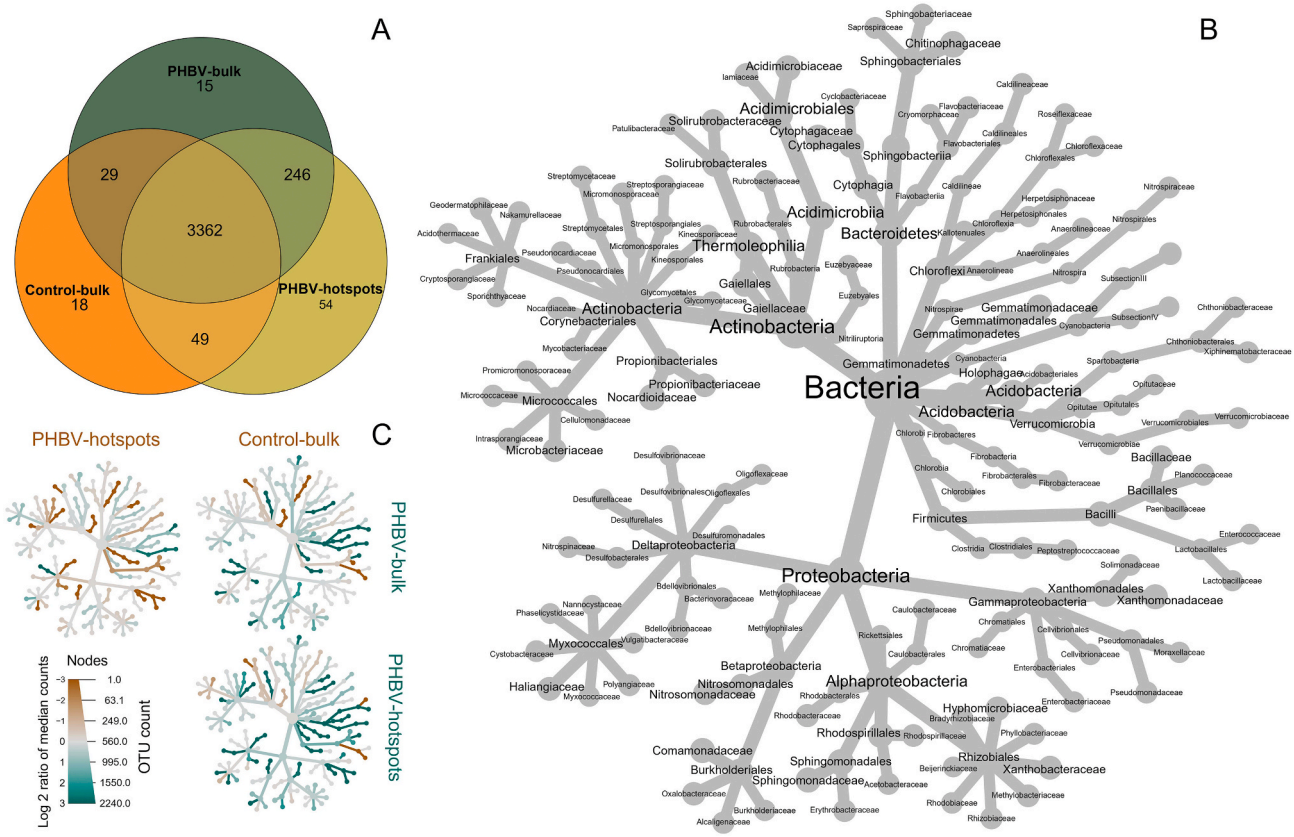

Fig. 5. Venn diagram shows shared number of OTUs by untreated soil (Control-bulk), and bulk (PHBV-bulk) and hotspots (PHBV-hotspots) soils with the bioplastic poly (3-hydroxybutyrate-*co*-3-hydroxyvalerate) (PHBV) addition (A). The taxonomical information for each node was given in an individual enlarged heatmap (B). Metacoder heatmap to family level across different treatment. Each node from the center (Kingdom) to outward (Family) represents different taxonomical levels (C). The map is weighted and colored-coded based on read abundance.

This contrasts with C hotpots in the rhizosphere, where the supply of C is probably less and where N is also lost from root epidermal cells in the form of amino acids providing a more balanced nutrient supply to the microbial community (Jones et al., 2009).

Here we speculate that PHBV breakdown was initially limited by the availability of polyhydroxybutyrate depolymerase (Jendrossek et al., 1993). The abundance and level of expression of this enzyme in soil remains unknown, however, an NCBI search revealed its presence in a wide range of microbial taxa. Although PHB depolymerase may be internally targeted (i.e. to break down internal storage C), there is also an evidence that it can be externally targeted (i.e. be an exoenzyme; Jendrossek and Handrick, 2002), probably to degrade microbial necromass (Handrick et al., 2004). Our data support the view that PHBV can be used as a sole C substrate by the bacterial community when supplied exogenously (Martinez-Tobon et al., 2018). However, we also observed a significant decrease (22%) in microbial specific growth rate μ in the microplastisphere compared to the rhizosphere, indicating the potential dominance of *K*-strategy microorganisms. *K*-strategists typically store more C in their cells and consume it slower (Nguyen and Guckert, 2001), lowering respiration rates. We therefore hypothesize that PHBV degraders break down PHBV exogenously into monomeric units which can then be subsequently transported into the cell where re-polymerization into PHB occurs (Shen et al., 2015). Consequently, microbial community structure in the microplastisphere shifted toward species with a lower affinity to oligosaccharides and peptides indicated by a higher K_m of β-glucosidase and leucine aminopeptidase.

4.3. Effect of PHBV on soil bacterial community structure

PHBV addition was associated with an increase in the relative abundance of *Acidobacteria, Proteobacteria* and *Chloroflexi*, and a decrease in the relative abundance of *Firmicutes*, The latter have previously been described as fast-growing copiotrophs that thrive in environments of high C availability (Cleveland et al., 2007; Jenkins et al., 2010). In contrast, *Acidobacteria* and *Chloroflexi* tend to dominate in oligotrophic environments where N availability is low (Ho et al., 2017). As mentioned, the release of high quantities of 3-hydroxybutyric acid during PHBV degradation may have also reduced the pH, thus favoring the growth of *Acidobacteria*. *Nitrospirae* are nitrite-oxidizing bacteria that are ubiquitous in terrestrial environments and that play a major role in biological N cycling and nitrification in agricultural soils (Xia et al., 2011). The higher abundance of *Nitrospirae* after PHBV addition indicated a change in N cycling (Zecchin et al., 2018), which was attributed to greater nutrient limitation in the microplastisphere than in the bulk soil (as indicated by V_{max} ratio of C-to-N cycling enzymes; 5.1 vs. 8.6) (Table S1). The relative proportion of *Bacteroidetes* also increased in the PHBV treatments. These largely copiotrophic organisms are widely distributed in soils, and are considered to be specialized in degrading complex organic matter (Huang et al., 2019). Thus, DOM pools increased in the PHBV-treated soil compared with bulk soil due to the release of monomeric compounds from PHBV degradation (Table 1). Although only bacterial communities were investigated in this study, it is likely that fungi and mesofauna populations are also greatly affected by PHBV addition and involved in its degradation. Further studies are required to gain a better insight into the complex interactions between these groups. Overall, our results highlight the potential of PHBV to trigger metabolic changes in soil microorganisms (Fig. 6), and thus potentially impact their functional role in soil (Huang et al., 2019). In addition to the microplastisphere, PHBV addition also changed the microbial community in the bulk soil, suggesting that these changes are not

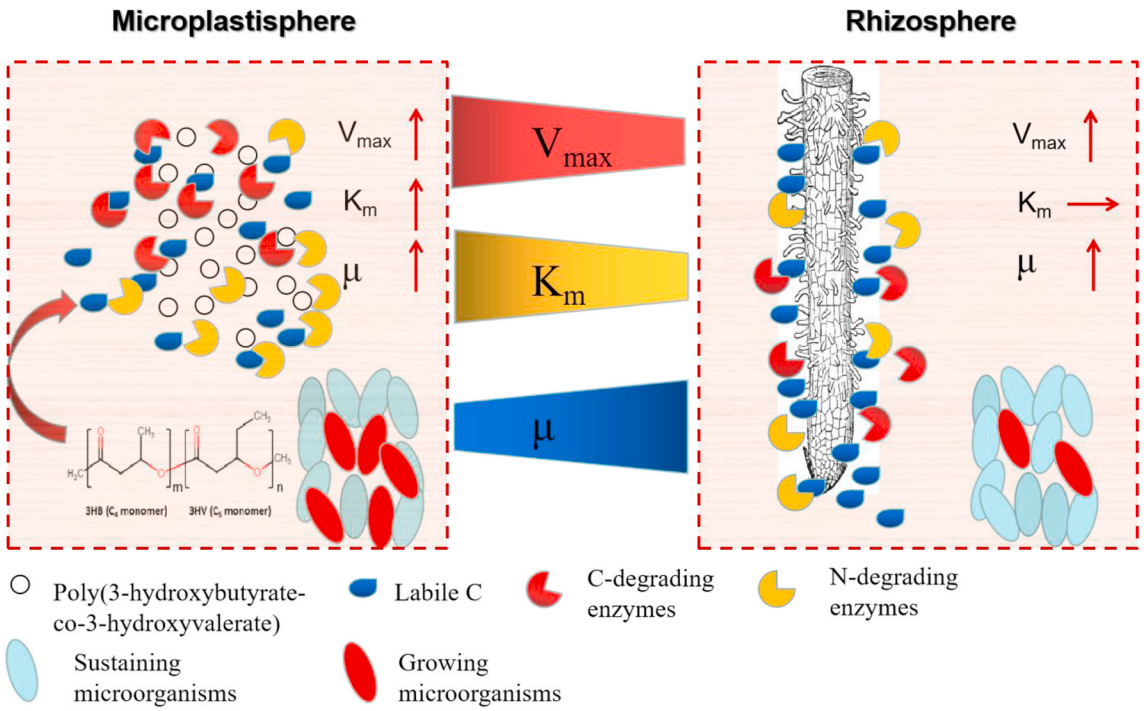

Fig. 6. Conceptual diagram showing changes of microbial activities and functions in the hotspots as affected by poly(3-hydroxybutyrate-*co*-3-hydroxyvalerate) (PHBV) addition. Vertical and horizontal red arrows indicate either an increase or no change of microbial exoenzyme kinetics and functions in the hotspots compared to the bulk soil, respectively. The red and orange gradient between the panels indicates the decreasing trend in enzyme activity (V_{max}) and substrate affinity (K_m), respectively between the microplastisphere and the rhizosphere. The blue gradient indicates the increasing trend in microbial specific growth rate (μ). (For interpretation of the references to color in this figure legend, the reader is referred to the Web version of this article.)

only confined to hotspots in the soil.

5. Conclusion

Microbial activity in agricultural soil is typically C-limited, such that even small C inputs can induce metabolic changes in the soil microbial community. Here we clearly showed that PHBV addition increased microbial activity, growth, and exoenzyme activity. This most likely leads to the enhanced mineralization of native SOM by co-metabolism, i.e. microorganisms degrade SOM by using degradable polymers as an energy source. Remarkably, greater enzyme activity and microbial biomass, and lower affinity for the substrate were observed in the microplastisphere compared to the rhizosphere, indicating a stronger and faster C and nutrient turnover with PHBV addition in hotspots. Taken together, the unique environment may benefit microbial survival in PHBV-treated soil compared with the rhizosphere, possibly altering the soil ecological functions and biogeochemical processes, which may result in a stimulation of soil C and nutrients cycling. Although bioplastics have been heralded as a solution to petroleum-based plastics, our research indicates that it is also important to consider the potential drawbacks of bioplastics, e.g., for plant growth and health. This is exemplified in the use of plastic microbeads in cosmetics and plastic mulch films in agriculture where the negative environmental consequences were only realized decades after their introduction (Sintim and Flurt, 2017; Qi et al., 2020b). Our research was designed to understand the short-term impact of a localized PHBV hotspot in soil. It is clear, however, that longer-term field-scale studies are also required. In-field testing of biodegradation of PHBV under different scenarios (e.g., soil types, agricultural practice, climate changes) as well as using a realistic mixture of polymers over longer periods is therefore required, with particular attention to plant-soil-microbial interactions.

Declaration of competing interest

The authors declare that they have no known competing financial interests or personal relationships that could have appeared to influence the work reported in this paper.

Acknowledgements

This work was supported by the China Agriculture Research System (CARS07-B-5) and the UKRI Global Challenges Research Fund (GCRF) project awarded to Bangor University (NE/V005871/1). We also would like to thank the UK-China Virtual Joint Center for Agricultural Nitrogen (CINAg, BB/N013468/1), which is jointly supported by the Newton Fund, via UK Biotechnology and Biological Sciences Research Council and Natural Environment Research Council, and the Chinese Ministry of Science and Technology. Jie Zhou would like to thank the support from the China Scholarship Council (CSC). Heng Gui would like to thank the National Natural Science Foundation of China (NSFC Grant 32001296) and Yunnan Fundamental Research Projects (Grant No. 2019FB063). The authors would like to thank Karin Schmidt for her laboratory assistance. The authors also thank the editor and two anonymous reviewers for their insightful comments.

Appendix A. Supplementary data

Supplementary data to this article can be found online at https://doi.org/10.1016/j.soilbio.2021.108211.

References

Allison, S.D., Weintraub, M.N., Gartner, T.B., Waldrop, M.P., 2011. Evolutionary economic principles as regulators of soil enzyme production and ecosystem function. In: Shukla, G., Varma, A. (Eds.), Soil Enzymology. Springer, Berlin, pp. 229–244.

Barnard, R.L., Osborne, C.A., Firestone, M.K., 2013. Responses of soil bacterial and fungal communities to extreme desiccation and rewetting. The ISME Journal 7, 2229–2241.
Blagodatskaya, E., Blagodatsky, S., Dorodnikov, M., Kuzyakov, Y., 2010. Elevated atmospheric CO_2 increases microbial growth rates in soil: results of three CO_2 enrichment experiments. Global Change Biology 16, 836–848.
Boots, B., Russell, C.W., Green, D.S., 2019. Effects of microplastics in soil ecosystems: above and below ground. Environmental Science and Technology 53, 11496–11506.
Bugnicourt, E., Cinelli, P., Lazzeri, A., Alvarez, V., 2014. Polyhydroxyalkanoate (PHA): review of synthesis, characteristics, processing and potential applications in packaging. Express Polymer Letters 8, 791–808.
Cleveland, C.C., Nemergut, D.R., Schmidt, S.K., Townsend, A.R., 2007. Increases in soil respiration following labile carbon additions linked to rapid shifts in soil microbial community composition. Biogeochemistry 82, 229–240.
de Souza Machado, A.A., Lau, C.W., Kloas, W., Bergmann, J., Bachelier, J.B., Faltin, E., Becker, R., Görlich, A.S., Rillig, M.C., 2019. Microplastics can change soil properties and affect plant performance. Environmental Science and Technology 53, 6044–6052.
Duis, K., Coors, A., 2016. Microplastics in the aquatic and terrestrial environment: sources (with a specific focus on personal care products), fate and effects. Environmental Sciences Europe 28, 2–8.
Edgar, R.C., Haas, B.J., Clemente, J.C., Quince, C., Knight, R., 2011. UCHIME improves sensitivity and speed of chimera detection. Bioinformatics 27, 2194–2200.
Fei, Y., Huang, S., Zhang, H., Tong, Y., Wen, D., Xia, X., Wang, H., Luo, Y., Barceló, D., 2020. Response of soil enzyme activities and bacterial communities to the accumulation of microplastics in an acid cropped soil. The Science of the Total Environment 707, 135634.
Fuller, S., Gautam, A., 2016. Procedure for measuring microplastics using pressurized fluid extraction. Environmental Science and Technology 50, 5774–5780.
Garrison, T.F., Murawski, A., Quirino, R.L., 2016. Bio-based polymers with potential for biodegradability. Polymers 8, 262.
German, D., Weintraub, M., Grandy, A., Lauber, C., Rinkes, Z., Allison, S., 2011. Optimization of hydrolytic and oxidative enzyme methods for ecosystem studies. Soil Biology and Biochemistry 43, 1387–1397.
Gross, R.A., Kalra, B., 2002. Biodegradable polymers for the environment. Science 297, 803–807.
Haider, T.P., Völker, C., Kramm, J., Landfester, K., Wurm, F.R., 2019. Plastics of the Future? The impact of biodegradable polymers on the environment and on society. Angewandte Chemie 58, 50–62.
Handrick, R., Reinhardt, S., Kimmig, P., Jendrossek, D., 2004. The "intracellular" poly(3-hydroxybutyrate) (PHB) depolymerase of *Rhodospirillum rubrum* is a periplasm-located protein with specificity for native PHB and with structural similarity to extracellular PHB depolymerases. Journal of Bacteriology 186, 7243–7253.
Ho, A., Di Lonardo, D.P., Bodelier, P.L.E, 2017. Revisiting life strategy concepts in environmental microbial ecology. FEMS Microbiology Ecology 93, fix006.
Hoang, D.T., Maranguit, D., Kuzyakov, Y., Razavi, B.S., 2020. Accelerated microbial activity, turnover and efficiency in the drilosphere is depth dependent. Soil Biology and Biochemistry 147, 107852.
Huang, Y., Zhao, Y., Wang, J., Zhang, M., Jia, W., Qin, X., 2019. LDPE microplastics films alter microbial community composition and enzymatic activities in soil. Environmental Pollution 254, 112983.
Jacquel, N., Lo, C.W., Wu, H.S., Wei, Y.H., Wang, S.S., 2007. Solubility of polyhydroxyalkanoates by experiment and thermodynamic correlations. AIChE Journal 53, 2704–2714.
Jambeck, J.R., Geyer, R., Wilcox, C., Siegler, T.R., Perryman, M., Andrady, A., Narayan, R., Law, K.L., 2015. Plastic waste inputs from land into the ocean. Science 347, 768–771.
Jan, M.T., Roberts, P., Tonheim, S.K., Jones, D.L., 2009. Protein breakdown represents a major bottleneck in nitrogen cycling in grassland soils. Soil Biology and Biochemistry 41, 2272–2282.
Jendrossek, D., Handrick, R., 2002. Microbial degradation of polyhydroxyalkanoates. Annual Review of Microbiology 56, 403–432.
Jendrossek, D., Knoke, I., Habibian, R.B., Steinbüchel, A., Schlegel, H.G., 1993. Degradation of poly(3-hydroxybutyrate), PHB, by bacteria and purification of a novel PHB depolymerase from *Comamonas* sp. Journal of Environmental Polymer Degradation 1, 53–63.
Jenkins, S.N., Rushton, S.P., Lanyon, C.V., Whiteley, A.S., Waite, I.S., Brookes, P.C., Kemmitt, S., Evershed, R.P., O'Donnell, A.G., 2010. Taxon-specific responses of soil bacteria to the addition of low level C inputs. Soil Biology and Biochemistry 42, 1624–163.
Jiang, Y., Chen, Y., Zheng, X., 2009. Efficient polyhydroxyalkanoates production from a waste-activated sludge alkaline fermentation liquid by activated sludge submitted to the aerobic feeding and discharge process. Environmental Science and Technology 43, 7734–7741.
Jones, D.L., Nguyen, C., Finlay, R.D., 2009. Carbon flow in the rhizosphere: carbon trading at the soil-root interface. Plant and Soil 32, 5–33.
Kujur, M., Patel, A.K., 2013. Kinetics of soil enzyme activities under different ecosystems: an index of soil quality. Chilean Journal of Agricultural Research 74, 96–104.
Kuzyakov, Y., 2010. Priming effects: interactions between living and dead organic matter. Soil Biology and Biochemistry 42, 1363–1371.
Kuzyakov, Y., Blagodatskaya, E., 2015. Microbial hotspots and hot moments in soil: concept & review. Soil Biology and Biochemistry 83, 184–199.
Lammirato, C., Miltner, A., Wick, L.Y., Kästner, M., 2010. Hydrolysis of cellobiose by β-glucosidase in the presence of soil minerals - interactions at solid - liquid interfaces and effects on enzyme activity levels. Soil Biology and Biochemistry 42, 2203–2210.
Liu, S., Razavi, B.S., Su, X., Maharjan, M., Zarebanadkouki, M., Blagodatskaya, E., Kuzyakov, Y., 2017. Spatio-temporal patterns of enzyme activities after manure application reflect mechanisms of niche differentiation between plants and microorganisms. Soil Biology and Biochemistry 112, 100–109.
Lucas, N., Bienaime, C., Belloy, C., Queneudec, M., Silvestre, F., Nava-Saucedo, J., 2008. Polymer biodegradation: mechanisms and estimation techniques. Chemosphere 73, 429–442.
Lopez-Hernandez, D., Lavelle, P., Niño, M., 1993. Phosphorus transformations in two P-sorption contrasting tropical soils during transit through *Pontoscolex corethrurus* (Glossoscolecidae: Oligochaeta). Soil Biology and Biochemistry 25, 789–792.
Mason-Jones, K., Banfield, C.C., Dippold, M.A., 2019. Compound-specific ^{13}C stable isotope probing confirms synthesis of polyhydroxybutyrate by soil bacteria. Rapid Communications in Mass Spectrometry 33, 795–802.
Martinez-Tobon, D.I., Gul, M., Elias, A.L., Sauvageau, D., 2018. Polyhydroxybutyrate (PHB) biodegradation using bacterial strains with demonstrated and predicted PHB depolymerase activity. Applied Microbiology and Biotechnology 102, 8049–8067.
Matavulj, M., Molitoris, H.P., 1992. Fungal degradation of polyhydroxyalkanoates and a semiquantitative assay for screening their degradation by terrestrial fungi. FEMS Microbiology Letters 103, 323–331.
Marx, M., Wood, M., Jarvis, S., 2001. A fluorimetric assay for the study of enzyme diversity in soils. Soil Biology and Biochemistry 33, 1633–1640.
Moorhead, D.L., Sinsabaugh, R.L., Hill, B.H., Weintraub, M.N., 2016. Vector analysis of ecoenzyme activities reveal constraints on coupled C, N and P dynamics. Soil Biology and Biochemistry 93, 1–7.
Napathorn, S.C., 2014. Biocompatibilities and biodegradation of poly(3-hydroxybutyrate-co-3-hydroxyvalerate)s produced by a model metabolic reaction-based system. BMC Microbiology 14, 285.
Nguyen, C., Guckert, A., 2001. Short-term utilisation of ^{14}C-glucose by soil microorganisms in relation to carbon availability. Soil Biology and Biochemistry 33, 53–60.
Obruca, S., Sedlacek, P., Krzyzanek, V., Mravec, F., Hrubanova, K., Samek, O., Kucera, D., Benesova, P., Marova, I., 2016. Accumulation of poly(3-hydroxybutyrate) helps bacterial cells to survive freezing. PloS One 11, e0157778.
Qi, R., Jones, D.L., Li, Z., Liu, Q., Yan, C., 2020a. Behavior of microplastics and plastic film residues in the soil environment: a critical review. The Science of the Total Environment 703, 134722.
Qi, Y.L., Yang, X.M., Pelaez, A.M., Lwanga, E.H., Beriot, N., Gertsen, H., Garbeva, P., Geissen, V., 2018. Macro- and micro- plastics in soil-plant system: effects of plastic mulch film residues on wheat (*Triticum aestivum*) growth. The Science of the Total Environment 645, 1048–1056.
Qi, Y., Ossowicki, A., Yang, X., Huerta Lwanga, E., Dini-Andreote, F., Geissen, V., Garbeva, P., 2020b. Effects of plastic mulch film residues on wheat rhizosphere and soil properties. Journal of Hazardous Materials 387, 121711.
Quast, C., Pruesse, E., Yilmaz, P., Gerken, J., Schweer, T., Yarza, P., Peplies, J., Glöckner, F.O., 2013. The SILVA ribosomal RNA gene database project: improved data processing and web-based tools. Nucleic Acids Research 41, 590–596.
Razavi, B.S., Zarebanadkouki, M., Blagodatskaya, E., Kuzyakov, Y., 2016. Rhizosphere shape of lentil and maize: spatial distribution of enzyme activities. Soil Biology and Biochemistry 96, 229–237.
Rillig, M.C., 2012. Microplastic in terrestrial ecosystems and the soil? Environmental Science and Technology 46, 6453–6454.
Rivera-Briso, A.L., Serrano-Aroca, Á., 2018. Poly(3-hydroxybutyrate-co-3-hydroxyvalerate): enhancement strategies for advanced applications. Polymers 10, 732.
Rochman, C.M., 2018. Microplastics research-from sink to source. Science 360, 28–29.
Saarma, K., Tarkka, M.T., Itavaara, M., Fagerstedt, K.V., 2003. Heat shock protein synthesis is induced by diethyl phthalate but not by di(2-ethylhexyl) phthalate in radish (*Raphanus sativus*). Journal of Plant Physiology 160, 1001–1010.
Sander, M., 2019. Biodegradation of polymeric mulch films in agricultural soils: concepts, knowledge gaps, and future research directions. Environmental Science and Technology 53, 2304–2315.
Shen, Y.C., Shaw, G.C., 2015. A membrane transporter required for 3-hydroxybutyrate uptake during the early sporulation stage in *Bacillus subtilis*. FEMS Microbiology Letters 362. UNSP fnv165.
Sintim, H.Y., Flury, M., 2017. Is biodegradable plastic mulch the solution to agriculture's plastic problem? Environmental Science and Technology 51, 1068–1069.
Song, X., Razavi, B., Ludwig, B., Zamanian, K., Zang, H., Kuzyakov, Y., Dippold, M., Gunina, A., 2020. Combined biochar and nitrogen application stimulates enzyme activity and root plasticity. The Science of the Total Environment 735, 139393.
Steinmetz, Z., Wollmann, C., Schaefer, M., Buchmann, C., David, J., Troger, J., Munoz, K., Fror, O., Schaumann, G.E., 2016. Plastic mulching in agriculture. Trading short-term agronomic benefits for -term soil degradation? The Science of the Total Environment 550, 690–705.
Vargas-Gastelum, L., Romero-Olivares, A.L., Escalante, A.E., Rocha-Olivares, A., Brizuela, C., Riquelme, M., 2015. Impact of seasonal changes on fungal diversity of a semi-arid ecosystem revealed by 454 pyrosequencing. FEMS Microbiology Ecology 91 fiv044.
Volova, T.G., Prudnikova, S.V., Vinogradova, O.N., Syrvacheva, D.A., Shishatskaya, E.I., 2017. Microbial degradation of polyhydroxyalkanoates with different chemical compositions and their biodegradability. Microbial Ecology 73, 353–367.
Wang, Q., Garrity, G.M., Tiedje, J.M., Cole, J.R., 2007. Naive Bayesian classifier for rapid assignment of rRNA sequences into the new bacterial taxonomy. Applied and Environmental Microbiology 73, 5261–5267.
Weithmann, N., Möller, J.N., Löder, M.G., Piehl, S., Laforsch, C., Freitag, R., 2018. Organic fertilizer as a vehicle for the entry of microplastic into the environment. Science Advances 4, 8060.

Wen, Y., Zang, H., Ma, Q., Evans, C.D., Chadwick, D.R., Jones, D.L., 2019. Is the 'enzyme latch' or 'iron gate' the key to protecting soil organic carbon in peatlands? Geoderma 349, 107–113.
Wen, Y., Freeman, B., Ma, Q., Evans, C., Chadwick, D., Zang, H., Jones, D., 2020. Raising the groundwater table in the non-growing season can reduce greenhouse gas emissions and maintain crop productivity in cultivated fen peats. Journal of Cleaner Production 262, 121179.
Xia, W., Zhang, C., Zeng, X., Feng, Y., Weng, J., Lin, X., 2011. Autotrophic growth of nitrifying community in an agricultural soil. The ISME Journal 5, 1226–1236.
Zang, H.D., Blagodatskaya, E., Wang, J.Y., Xu, X.L., Kuzyakov, Y., 2017. Nitrogen fertilization increases rhizodeposit incorporation into microbial biomass and reduces soil organic matter losses. Biology and Fertility of Soils 53, 419–429.
Zang, H., Blagodatskaya, E., Wen, Y., Xu, X., Kuzyakov, Y., 2018. Carbon sequestration and turnover in soil under the energy crop Miscanthus: repeated ^{13}C natural abundance approach and literature synthesis. Global Change Biology Bioenergy 10, 262–271.
Zang, H., Wang, J., Kuzyakov, Y., 2016. N fertilization decreases soil organic matter decomposition in the rhizosphere. Applied Soil Ecology 108, 47–53.
Zang, H., Xiao, M., Wang, Y., Ling, N., Wu, J., Ge, T., Kuzyakov, Y., 2019. Allocation of assimilated carbon in paddies depending on rice age, chase period and N fertilization: experiment with $^{13}CO_2$ labelling and literature synthesis. Plant and Soil 445, 113–123.
Zang, H., Zhou, J., Marshall, M.R., Chadwick, D.R., Wen, Y., Jones, D.L., 2020. Microplastics in the agroecosystem: are they an emerging threat to the plant-soil system? Soil Biology and Biochemistry 148, 107926.
Zecchin, S., Mueller, R.C., Seifert, J., Stingl, U., Anantharaman, K., von Bergen, M., Cavalca, L., Pester, M., 2018. Rice paddy Nitrospirae carry and express genes related to sulfate respiration: proposal of the new genus "*Candidatus Sulfobium*". Applied and Environmental Microbiology 84 e02224-17.
Zettler, E.R., Mincer, T.J., Amaral-Zettler, L.A., 2013. Life in the "plastisphere": microbial communities on plastic marine debris. Environmental Science and Technology 47, 7137–7146.
Zhang, X., Kuzyakov, Y., Zang, H., Dippold, M.A., Shi, L., Spielvogel, S., Razavi, B.S., 2020. Rhizosphere hotspots: root hairs and warming control microbial efficiency, carbon utilization and energy production. Soil Biology and Biochemistry 107872.
Zimmermann, L., Dierkes, G., Ternes, T.A., Volker, C., Wagner, M., 2019. Benchmarking the in vitro toxicity and chemical composition of plastic consumer products. Environmental Science and Technology 53, 11467–11477.
Zhou, J., Wen, Y., Shi, L.L., Marshall, M.R., Kuzyakov, Y., Blagodatskaya, E., Zang, H.D., 2020a. Strong priming of soil organic matter induced by frequent input of labile carbon. Soil Biology and Biochemistry 152, 108069.
Zhou, J., Zang, H., Loeppmann, S., Gube, M., Kuzyakov, Y., Pausch, J., 2020b. Arbuscular mycorrhiza enhances rhizodeposition and reduces the rhizosphere priming effect on the decomposition of soil organic matter. Soil Biology and Biochemistry 140, 107641.
Zinn, M., Witholt, B., Egli, T., 2001. Occurrence, synthesis and medical application of bacterial polyhydroxyalkanoate. Advanced Drug Delivery Reviews 253, 5–21.